Mass Transfer of CO_2 in A Carbonated Water-Oil System at High Pressures

Guanli Shu, Mingzhe Dong[*], Shengnan Chen, Hassan Hassanzadeh

Department of Chemical and Petroleum Engineering, Schulich School of Engineering,

University of Calgary, 2500 University Drive NW, Calgary, AB, Canada T2N 1N4

[*] Corresponding author. Email: mingzhe.dong@ucalgary.ca (M Dong).

1. DETERMINATION OF PHASE DENSITY

During the mass transfer of CO_2 from the carbonated water into the oil, the densities of the water and oil phases will be altered. The changes of densities are relevant to the alterations of pressure and to the CO_2 concentrations at the experimental temperature. In the following subsections, phase behavior simulator CMG Winprop[1] is used to calculate densities of oil and water phases at different pressures and different CO_2 concentrations. Peng Robinson equation of state is applied for the thermodynamic modelling. The determined densities are correlated based on the method proposed by Li et al. (2004)[2] for calculating water and oil densities at a desired pressure and CO_2 concentration in using the developed analytical model to estimate CO_2 diffusion coefficients in the carbonated water-oil system. For determination of partition coefficient, the same procedure is followed except that concentrations of CO_2 in water and oil phases are calculated instead of densities.

1.1. Density of water phase. For the studied system, carbonated water is formed by dissolving CO_2 into brine with a salinity of 3.0 wt% at a desired pressure and temperature. The density of the CO_2 + brine solution is of importance in determining the diffusion coefficients. To simplify the trial-and-error procedure, the correlation of the density of the water phase can be determined in terms of the method reported by Li et al.[2] Table S1 lists the densities of the CO_2 + brine solutions at 20℃. In this table, the data shown in the first row (in bold) are densities corresponding to indicated saturation pressures (4 MPa, 6 MPa, 10 MPa, 16 MPa, and 20 MPa). The data in the second column represent densities of brine without the dissolution of CO_2 corresponding to pressures indicated in the first column.

Table S1. Calculated densities of CO_2 + brine solutions at 20℃

| P (MPa)	ρ^* (g/cm^3)	P (MPa)	ρ (g/cm^3)	P (MPa)	ρ (g/cm^3)	P (MPa)	ρ (g/cm^3)	P (MPa)	ρ (g/cm^3)	P (MPa)	ρ (g/cm^3)
0.1	1.0195	**4**	**1.0290**	**6**	**1.0313**	**10**	**1.0343**	**16**	**1.0374**	**20**	**1.0392**
2	1.0204	6	1.0299	10	1.0330	12	1.0351	18	1.0382	22	1.0400
4	1.0213	10	1.0316	14	1.0347	14	1.0360	20	1.0390	24	1.0408
6	1.0222	14	1.0333	18	1.0364	18	1.0376	22	1.0398	26	1.0416
10	1.0239	18	1.0349	20	1.0372	20	1.0385	24	1.0407	28	1.0424
14	1.0256	20	1.0358	24	1.0388	24	1.0401	26	1.0415	30	1.0432
18	1.0274	24	1.0374								
20	1.0282										
24	1.0299										

* Density of brine without dissolution of CO_2.

Figure S1 shows the density results from Table S1 as a function of pressure for different CO_2 concentrations. In this figure, the curve with diamonds stands for the densities of brine without CO_2 dissolution (i.e., C = 0); the curve with solid circles indicates the densities of CO_2 saturated brine solutions at different saturation pressures; the other curves represent the densities of unsaturated brine solutions with different CO_2 concentrations (C = 0.9262×10^{-3} ~ 1.3575×10^{-3} mol/cm^3). As illustrated in Figure S1, for a given CO_2 concentration, the density of the brine solution increases linearly with pressure. Of note is that these curves follow almost the same slope. From another perspective, it can be seen that the density of the brine solution increases alongside the increase of the CO_2 concentration at a given pressure. In other words, the dissolution of carbon dioxide increases the density of the aqueous phase.
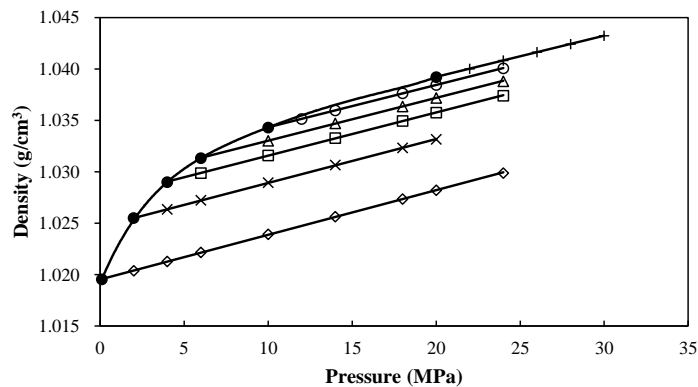
Figure S1. Density of CO_2 + brine solution versus pressure with different CO_2 concentrations at 20℃: ◇, brine, C = 0; ×, C = 0.6076×10^{-3} mol/cm^3; □, C = 0.9262×10^{-3} mol/cm^3; Δ, C =

$1.1009{\times}10^{-3}$ mol/cm³; ○, C = $1.2587{\times}10^{-3}$ mol/cm³; +, C = $1.3575{\times}10^{-3}$ mol/cm³; and ●, at different saturation pressures.
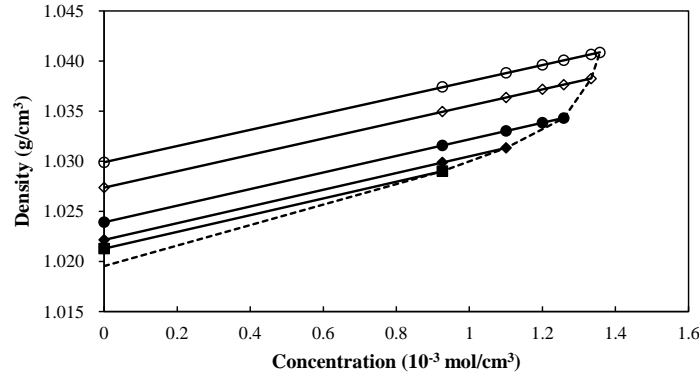
Figure S2. Density of CO_2 + brine solution versus CO_2 concentration under selected pressures at 20°C: ■, 4 MPa; ◆, 6 MPa; ●, 10 MPa; ◇, 18 MPa; ○, and 24 MPa.

As shown in Figure S2, the densities of the CO_2 + brine solution at different pressures (4 - 24 MPa) are plotted as a function of the CO_2 concentration at 20°C. In this figure, the intercept of each curve represents the density of the brine without CO_2 dissolution. The end point (right-most value) for each curve represents the density of the CO_2 saturated brine solution at the corresponding saturation pressure. It can be concluded from this figure that the density of the brine solution upon dissolving CO_2 increases linearly as the CO_2 concentration increases at a given pressure. In addition, all of the curves very nearly follow the same slope. As reported by Li et al.,[2] based on the results shown in Figures S1 and S2, the density of the CO_2 + brine solution can be calculated by eqs S1 and S2:

$$\rho_{ws} = \rho_p + \beta C, \qquad\qquad 0 \leq C \leq C_{sat} \qquad\qquad\qquad (S1)$$

$$\rho_p = \rho_0 + \alpha P \qquad\qquad\qquad (S2)$$

where ρ_{ws} is the density of the CO_2 + brine solution at a certain concentration and pressure; ρ_p is the density of the water phase without dissolution of the CO_2 at a given pressure (P), g/cm³; C is the concentration of CO_2 in the CO_2 + brine solution, mol/cm³; C_{sat} is the CO_2 solubility in brine at the corresponding pressure (P), mol/cm³; β is the slope of density versus concentration in Figure S2, g/mol; α is the slope of the curve for brine without CO_2 (i.e., the slope of curve with

S4

diamonds in Figure S1), g/(cm^3·MPa); and ρ_0 is the intercept of the curve for brine without CO_2 (i.e., the slope of curve with diamonds in Figure S1), g/cm^3. The values of β, α, and ρ_0 for the water system have been listed in Table S2. Therefore, the density of CO_2 + brine solution at any pressure and CO_2 concentration at 20°C can be determined from the following correlation:

$$\rho_{ws} = (1.0195 + 0.00043\,P) + 8.23\,C \tag{S3}$$

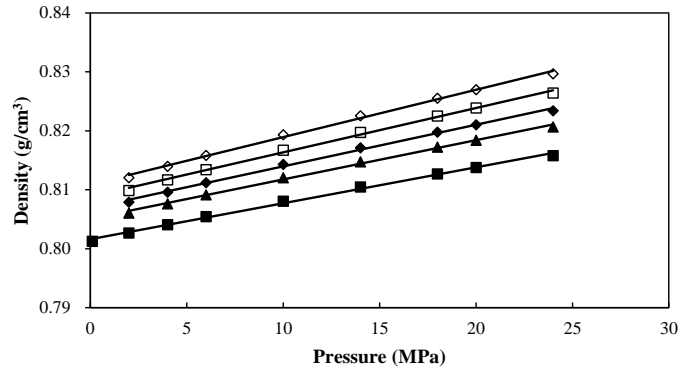**Table S2**. Values of parameters in eqs S1 and S2 for brine and crude oil systems

Fluid	β (g/mol)	α (g/(cm^3·MPa))	ρ_0 (g/cm^3)
Brine	8.23	0.00043	1.0195
Crude oil	7.60	0.00061	0.8013

1.2. Density of oil phase. In the process of the CO_2 mass transfer from the carbonated water phase into the oil phase, the density of the CO_2 + crude oil system will be changed. Thus, it is vital to correlate the density change as a function of the CO_2 concentration and pressure in order to facilitate the trial and error procedure. The same method of determining the density of the CO_2 + brine solution as discussed above has been applied to the density of the CO_2 + crude oil system. The properties of crude oil are listed in the Materials and Method section. The densities of the CO_2 + crude oil mixture at 20°C are listed in Table S3. The data appearing in the first row (in bold) are the initial CO_2 concentrations at 2 MPa. The data in the second column represent densities of crude oil without the dissolution of CO_2 corresponding to pressures indicated in the first column. The selected concentrations and pressures cover the actual experimental CO_2 concentrations and pressures. To better understand the density changes of the CO_2 + crude oil mixture, Figures S3 and S4 are plotted based on the results in Table S3. In each of these figures, the curve with solid squares indicates the densities of the crude oil without CO_2 dissolution (i.e., C=0); the other curves in each figure represent the densities of unsaturated crude oils with different CO_2 concentrations (C=0.5366×10^{-3} - 1.5320×10^{-3} mol/cm^3).

Table S3. Densities of CO_2 + crude oil at 20℃

C=0 mol/cm³		C=0.5366×10⁻³ mol/cm³		C=0.8397×10⁻³ mol/cm³		C=1.1702×10⁻³ mol/cm³		C=1.5320×10⁻³ mol/cm³	
P (MPa)	ρ (g/cm3)	P (MPa)	ρ (g/cm3)	P (MPa)	ρ (g/cm3)	P (MPa)	ρ (g/cm3)	P (MPa)	ρ (g/cm3)
0.1	0.8013	**2**	**0.8060**	**2**	**0.8079**	**2**	**0.8099**	**2**	**0.8120**
2	0.8027	4	0.8076	4	0.8096	4	0.8117	4	0.8140
4	0.8041	6	0.8092	6	0.8112	6	0.8134	6	0.8158
6	0.8055	10	0.8121	10	0.8143	10	0.8167	10	0.8193
10	0.8081	14	0.8147	14	0.8171	14	0.8197	14	0.8226
14	0.8105	18	0.8172	18	0.8198	18	0.8225	18	0.8256
18	0.8127	20	0.8184	20	0.8210	20	0.8239	20	0.8270
20	0.8138	24	0.8207	24	0.8234	24	0.8264	24	0.8297
24	0.8158								

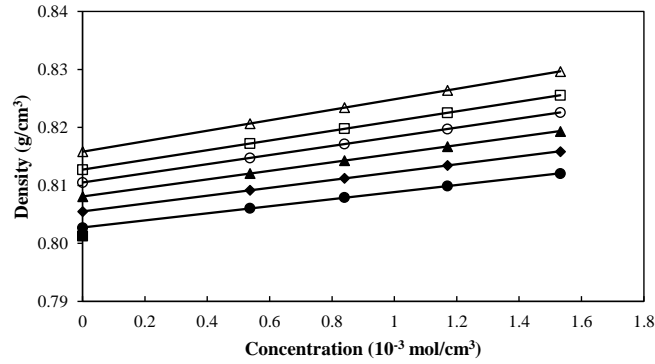**Figure S3.** Density of CO_2 + crude oil versus pressure with different CO_2 concentrations at 20℃: ■, without CO_2, C=0; ▲, C=0.5366×10⁻³ mol/cm³; ◆, C=0.8397×10⁻³ mol/cm³; □, C=1.1702×10⁻³ mol/cm³; and ◇, C=1.5320×10⁻³ mol/cm³.

From Figure S3, it can be observed that the crude oil becomes denser as pressure increases for a given CO_2 concentration in good linear relationships. Moreover, all the curves are reasonably parallel with similar slopes. Thus, for a given pressure, it is apparent that the density of the crude oil mixture increases as the CO_2 concentration increases as a result of the mass transfer of CO_2 from the carbonated water into crude oil. Figure S4 describes the density of the CO_2 + crude oil system as a function of the CO_2 concentration and parameterized by pressure. The intercept of each curve represents the density of crude oil without CO_2 dissolution (i.e., C=0). Analogously, it can be seen that good linear relationships exist for all conditions. Following the same method, the values of parameters for crude oil have been listed in Table S2. The density of the

CO_2 + crude oil mixture can be calculated using the following correlation equation (eq S4):

$$\rho_{om} = (0.8013 + 0.00061\,P) + 7.60\,C \tag{S4}$$

where ρ_{om} is the density of the CO_2 + crude oil mixture, g/cm^3; and C is the CO_2 concentration, mol/cm^3.

Figure S4. Density of CO_2 + crude oil versus CO_2 concentration under selected pressures at 20℃. ■, 0.1 MPa; ●, 2 MPa; ◆, 6 MPa; ▲, 10 MPa; ○, 14 MPa; □, 18 MPa; and △, 24 MPa.


2. DETERMINATION OF PARTITION COEFFICIENT

Considering that the concentrations of CO_2 at the interface in the water and oil phases will vary with time, the values of the interface concentrations need to be determined along with the diffusion coefficients. To reduce the complexity of obtaining interface concentrations, the approach of determining a partition coefficient (k_{pc}) is adopted. In view of the different solubilities of CO_2 in water and oil phases, CO_2 concentrations at the interface will have an important impact on the mass transfer process. This concentration difference can be described by means of a partition coefficient. Here, the partition coefficient is defined as the ratio of the concentration of carbon dioxide in the oil phase divided by that in the water phase, and it is therefore dimensionless. Considering the partition coefficient is a function of pressure, temperature, and CO_2 concentration, it is imperative to establish a correlation relationship to simplify the trial-and-error procedure. In this work, the studied temperature is kept at 20℃; thus, only two parameters need to be considered. At the same time, we consider the mass transfer process of the CO_2 from the carbonated water into the oil. The CO_2 is initially dissolved only in the water phase and there is no CO_2 in the oil phase. A commercial phase equilibrium software

package (CMG Winprop[1]) is applied to determine the equilibrium concentrations of CO_2 in the water and oil phases under different pressures. Table S4 shows the partition coefficients of CO_2 in the water-CO_2-oil system at 20℃. In this table, the data shown in the first row (in bold) represent the conditions at which the brine is fully saturated at different saturation pressures (4 MPa, 6 MPa, 10 MPa, 14 MPa, 18 MPa, and 22 MPa).

Table S4. Partition coefficients of CO_2 in the water-CO_2-oil system with different initial CO_2 concentrations in the water phase at 20℃

P (MPa)	k_{pc}	P (MPa)	k_{pc}	P (MPa)	k_{pc}	P (MPa)	k_{pc}	P (MPa)	k_{pc}	P (MPa)	k_{pc}
4	**3.361**	**6**	**3.397**	**10**	**3.399**	**14**	**3.367**	**18**	**3.328**	**22**	**3.290**
6	3.332	10	3.342	14	3.347	18	3.319	20	3.306	24	3.269
10	3.278	14	3.291	18	3.300	20	3.297	22	3.284	26	3.249
14	3.228	18	3.244	20	3.277	22	3.275	24	3.263	28	3.230
18	3.183	20	3.222	24	3.235	24	3.254	26	3.243	30	3.211
20	3.161	24	3.181	26	3.215	26	3.234	28	3.224		
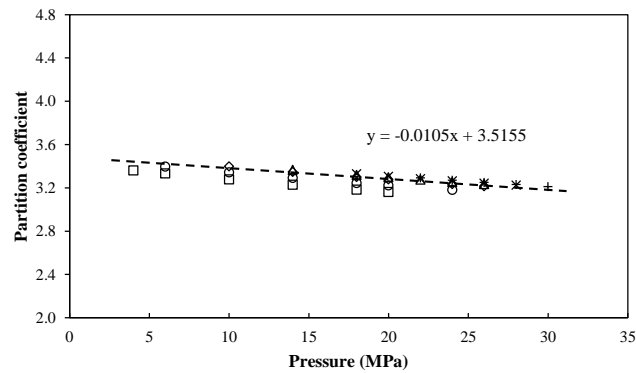
Figure S5. Partition coefficients of CO_2 in the water-CO_2-oil system with different initial CO_2 concentrations in the water phase at 20℃. □, $C=0.9170\times10^{-3}$ mol/cm³; ○, $C=1.0950\times10^{-3}$ mol/cm³; ◇, $C=1.2570\times10^{-3}$ mol/cm³; △, $C=1.3170\times10^{-3}$ mol/cm³; ×, $C=1.3470\times10^{-3}$ mol/cm³; and +, $C=1.3700\times10^{-3}$ mol/cm³.

Figure S5 shows the partition coefficient as a function of pressure and CO_2 concentration based upon the results from Table S4. The symbols of square, circle, diamond, triangle, cross,

and plus marks stand for conditions with different initial concentrations of CO_2 in the water phase. From this figure, it can be observed that the changes in the partition coefficient are quite small as the CO_2 concentration increases at a given pressure. For this reason, the partition coefficient can be considered to be independent of concentration. However, for a given concentration, the coefficient decreases as the pressure increases. An averaged correlation between the partition coefficient and pressure can be determined as:

$$k_{pc} = -0.0105\,P + 3.5155 \tag{S5}$$

where k_{pc} is the partition coefficient, dimensionless; and P is the experimental pressure, MPa.

3. EFFECT OF NUMBER OF SUBINTERVALS IN DETERMINATION OF DIFFUSION COEFFICIENTS

In the procedure of diffusion coefficient estimation, the domains (oil and water phases) were discretized into a number of subintervals. It turns out that the number of subintervals used for the oil and water domains can affect the estimated diffusion coefficient; specifically, an inappropriate selection of the number of intervals results in inaccurate results. In this study, based on the CO_2 concentration distribution profile, diffusion coefficients of carbon dioxide in the water and oil phases are determined by minimization of the differences of the phase volumes and diffusion fluxes, using a trial-and-error procedure. Consequently, it is necessary to study the effect of subintervals on the estimated diffusion coefficients so as to optimize the number of intervals and minimize the estimation error. Table S5 shows the calculated diffusion coefficients of carbon dioxide in the water and oil phases at 17.19 MPa (at 10 hours) and 20°C (Test 1), showing the effect of choosing different numbers of subintervals. The results shown in Figure S6 reveal that using a small number of subintervals (less than 10) underestimates the diffusion coefficients for both water and oil phases. As the number of subintervals increases, the estimated diffusion coefficients tend to converge to a constant value. Taking into account the computation time and the acceptable convergences achieved, the optimal number of 10 subintervals is used in the analysis.

Table S5. Comparison of the effect of subintervals on calculated diffusion coefficients of carbon dioxide in water and oil phases at 17.66 MPa and at temperature of 20˚C (Test 1)

Number of subintervals	Phase volume determined (cm^3)			Diffusion coefficients		Different of phase volumes (cm^3)	Difference of diffusion fluxes ($mol/(cm^2 \cdot s)$)
	Water	Oil	Total	D_w (10^{-5} cm^2/s)	D_o (10^{-6} cm^2/s)		
1	79.845	70.177	150.022	0.94	0.96	0.022	2.98×10^{-11}
5	79.841	70.181	150.022	0.98	1.00	0.022	1.95×10^{-11}
10	79.839	70.183	150.022	1.00	1.02	0.022	5.02×10^{-12}
15	79.840	70.182	150.022	1.00	1.02	0.022	5.02×10^{-12}
20	79.838	70.177	150.015	1.00	1.02	0.015	8.41×10^{-12}
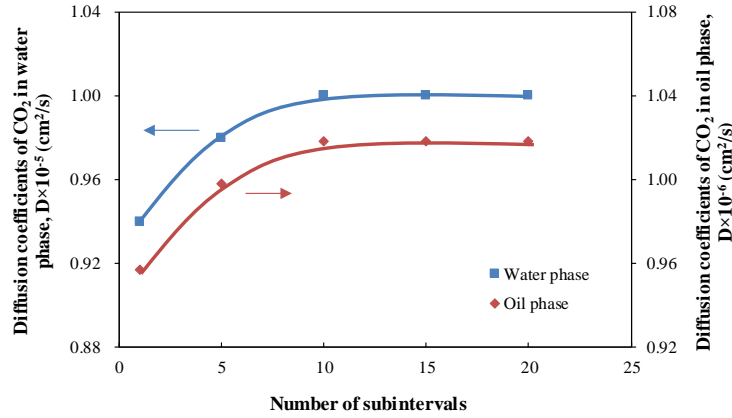
Figure S6. Effect of number of subintervals on calculated diffusion coefficients of CO_2 in water and oil phase at 17.66 MPa and at temperature of 20˚C (Test 1).

4. DETERMINATION OF OPTIMAL DIFFUSION COEFFICIENTS

The developed analytical model and the trial-and-error procedure described in the previous section are used to estimate the diffusion coefficients of carbon dioxide in carbonated water and oil phases. In this analysis, the results obtained from Test 1 are chosen as an example to elucidate the feasibility of applying the proposed methodology. The pressure builds up in the diffusion cell for Test 1 has been shown in Figure 7, shown in the paper. Based upon this pressure data, diffusivities are determined at 10 hours. The experimental pressure at 10 hours is 17.19 MPa. Parameters at the initial condition for this test are listed in Table 2 (shown in the paper).

Table S6 demonstrates several sets of the estimated diffusion coefficients which satisfy the two convergence criteria for Test 1. However, the optimum diffusion coefficients need to be determined such that the difference in the estimated flux in both phases is at a minimum. In other words, a set that results in minimum flux differential needs to be identified among all converged sets. From this table, it can be seen that interface concentrations have a great impact on the determination of diffusion coefficients. The unreasonable guesses of interface concentrations lead to overestimated or underestimated diffusivities. Another important point is that the interface concentration of CO_2 in the oil phase is greater than that in the water phase. This is because the concentration partition between two phases at the interface is directly affected by the solubility of CO_2 and is governed by the partition coefficient, as discussed in the previous section. To better elucidate the procedure of finding the optimal diffusion coefficients, Table S6 and Figure S7 are combined. As shown in Table S6, compared to the moderate variations of the difference in the phase volumes, the difference in the diffusion fluxes seems to be significant. It can be intuitively seen from Figure S7 that there exists an interface concentration C_w^* at which the difference in the fluxes is a minimum, occurring at $C_w^* = 0.65\times10^{-3}$ mol/cm^3. As a result, the values of the interface concentrations (C_w^* and C_o^*) and diffusion coefficients (D_o and D_w) determined at the interface concentration of 0.65×10^{-3} mol/cm^3 in the water phase shall be selected as the optimum results (i.e., Set 12).

Table S6. Six sets of estimated interface concentrations and diffusion coefficients satisfying the convergence criteria for Test 1 at 10 hours under 20°C

Set No.	Estimated concentration of CO_2 at the interface, 10^{-3} (mol/cm^3)		Concentration difference of CO_2 at the interface between water and oil phases, 10^{-3} (mol/cm^3)	Estimated diffusion coefficients (cm^2/s)		Difference of phase volume changes (cm^3)	Difference of diffusion fluxes (mol/(cm^2·s))
	C_w^*	C_o^*		D_w	D_o		
1	0.75	2.50	1.75	1.50×10^{-5}	8.31×10^{-7}	0.025	2.37×10^{-10}
2	0.70	2.33	1.63	1.10×10^{-5}	8.27×10^{-7}	0.021	1.45×10^{-10}
7	0.60	2.00	1.40	1.00×10^{-5}	1.38×10^{-6}	0.025	1.15×10^{-10}
10	0.54	1.78	1.24	1.00×10^{-5}	2.09×10^{-6}	0.028	2.14×10^{-10}
11	0.50	1.67	1.17	1.00×10^{-5}	2.59×10^{-6}	0.029	2.52×10^{-10}
12	0.65	2.17	1.52	1.00×10^{-5}	1.02×10^{-6}	0.022	5.02×10^{-12}
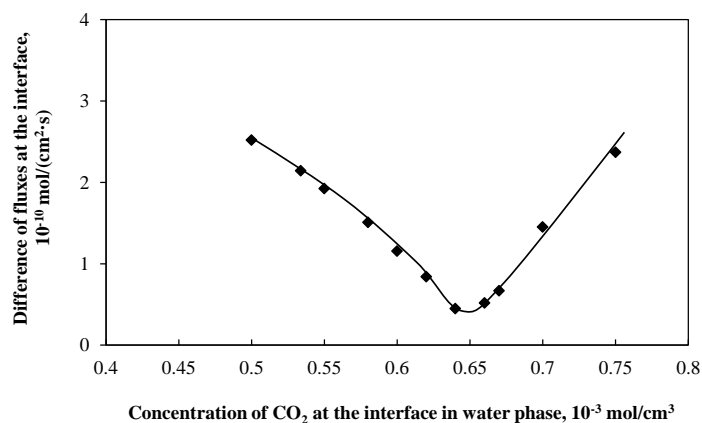
Figure S7. Comparison of the differences of diffusion fluxes at the interface in water and oil phases as a function of concentration of CO_2 at the interface in the water phase.

REFERENCES

(1) Compter Modeling Group Ltd. *Winprop User's Guide*; Computer Modelling Group Ltd.; Calgary, Alberta, Canada, 2013.

(2) Li, Z.; Dong, M.; Li, S.; Dai, L. Densities and Solubilities for Binary Systems of Carbon Dioxide + Water and Carbon Dioxide + Brine at 59 °C and Pressures to 29 MPa. *J. Chem. Eng. Data* **2004**, *49*, 1026-1031.